

DIFFÉRENTS VISAGES DE LA TRIBOLOGIE
DIFFERENT FACES OF TRIBOLOGY

Low-velocity friction between macroscopic solids

Lionel BUREAU, Tristan BAUMBERGER, Christiane CAROLI, Oliver RONSIN

Groupe de physique des solides¹, 2, place Jussieu, 75251 Paris cedex 05, France
E-mail: bureau@gps.jussieu.fr

(Reçu le 23 février 2001, accepté le 23 février 2001)

Abstract. We analyze the physical mechanisms taking place in unlubricated friction between surfaces of micrometric roughness at sliding speeds $< 100 \mu\text{m}\cdot\text{s}^{-1}$. This analysis is based on extensive experimental investigations of the time and velocity dependences of static and dynamic friction forces, and of non-stationary sliding. It fully supports the state and rate dependent friction model first proposed by Rice and Ruina. © 2001 Académie des sciences/Éditions scientifiques et médicales Elsevier SAS

friction / ageing / rheology

Frottement solide basse vitesse

Résumé. Nous présentons une analyse des mécanismes physiques responsables du frottement d'un contact non lubrifié entre des surfaces de rugosité micrométrique, à des vitesses de glissement inférieures à $100 \mu\text{m}\cdot\text{s}^{-1}$. Cette analyse s'appuie sur de multiples études expérimentales des dépendances en temps et en vitesse des forces de frottement statique et dynamique, ainsi que du glissement non stationnaire. Elle justifie pleinement le modèle de frottement « state and rate dependent » proposé par Rice et Ruina. © 2001 Académie des sciences/Éditions scientifiques et médicales Elsevier SAS

frottement / vieillissement / rheologie

1. Introduction

When two macroscopic solids are brought into contact, they exhibit a resistance to relative motion, known as solid friction, first extensively studied by Amontons (1699) and Coulomb (1781). Their description of friction is still widely used nowadays.

Consider a solid block slider pressed against a flat horizontal track under a normal force W . Let F be the pulling force applied on the slider, parallel to the contact surface of nominal area Σ_0 (figure 1a).

Starting from rest, a minimum force $F_s = \mu_s W$ is needed to move the slider: μ_s is called the static friction coefficient. Once a steady sliding state at velocity V is achieved, the pulling force $F = \mu_d W$, where μ_d is the dynamic friction coefficient.

The Amontons–Coulomb laws state that:

- μ_s and μ_d are independent of the force W and the nominal area Σ_0 ;
- usually, $\mu_d < \mu_s$.

Note présentée par Guy LAVAL.

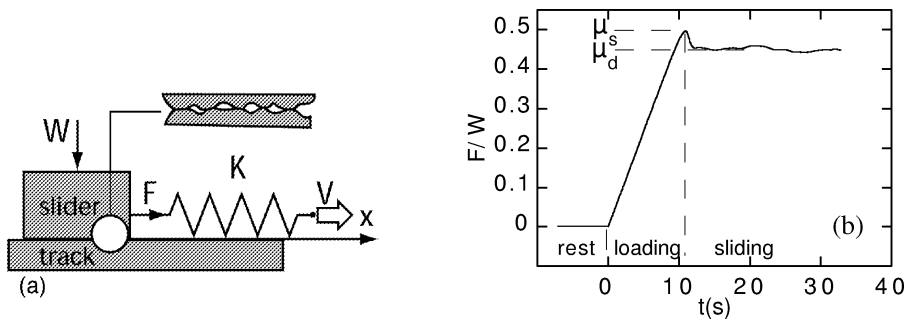


Figure 1. (a) Schematic setup: the end of the loading spring (stiffness K) is driven at constant velocity V . The normal load is W and the tangential force applied to the slider is F . The surface roughness is responsible for the multicontact nature of the interface. (b) Ratio F/W as a function of time when driving the end of the loading spring at constant velocity $V = 10 \mu\text{m}\cdot\text{s}^{-1}$. The ratio reaches a maximum value μ_s and then drops to its steady sliding value μ_d .

The basic question is then to understand the physical mechanisms underlying these macroscopic laws of friction.

In their pioneer work [1], Bowden and Tabor (BT) emphasized the role played by surface roughness. Indeed, surfaces of macroscopic solids, though nominally flat, exhibit a roughness typically on the micrometric order. Hence, when the solids are in contact, the real area Σ_r over which the contact effectively occurs is only a small fraction of the nominal area Σ_0 . The interface between the two solids, that will be referred to as a multicontact interface, consisting of a large number of dilute micrometric contacts between asperities.

BT then postulated the existence of a stress σ_s , characteristic of the shear strength of the interface. The friction force F thus reads:

$$F = \sigma_s \Sigma_r \quad (1)$$

In this approach, the Amontons–Coulomb law $F = \mu W$ amounts to stating that the real area of contact Σ_r is proportional to W . Moreover, BT pointed out that since $\Sigma_r \ll \Sigma_0$, for metal/metal interfaces, the local pressure on the contacts is comparable with the yield stress of the contacting materials, resulting in a plastic deformation of the load bearing asperities.

Greenwood [2] later extended this analysis, in the framework of a statistical description of random surface profiles, to the case of non fully plastic asperity deformation (e.g. elastomers, glasses), and drew the following conclusions:

- (i) the number of contacts $N \propto W$;
- (ii) the mean contact size $\langle a \rangle$ is independent of W ;
- (iii) hence $\Sigma_r \propto W$.

These features hold for an interface for which the number of contacts N is large enough for a statistical approach to be valid, and the fraction $\Sigma_r/\Sigma_0 \ll 1$ for the contacts to be elastically independent.

Nevertheless, the classical Amontons–Coulomb laws reveal too little to account properly for the complex sliding dynamics of a multicontact interface. For instance, stick–slip oscillations, responsible for squeaks, string music or earthquakes, cannot be described within this basic framework.

We present in this article the picture of the physical mechanisms at work in unlubricated solid friction at a multicontact interface, as it has emerged from recent experimental investigations and phenomenology [3–7]. These experiments have been conducted on the setup sketched in figure 1a, composed of a slider driven along a track through a loading spring. Two main regimes can be distinguished:

- For tangential forces $F \ll F_s$, the interface is *pinned*. In agreement with the Amontons–Coulomb description of the static regime, no irreversible motion occurs, though careful measurements of submicronic displacements reveal a linear elastic response.

- When the slider is pulled at constant velocity V , it may either perform steady sliding at V , or stick–slip oscillations, depending on the value of V and of the stiffness of the loading system.

The static and sliding regimes are separated by the static threshold, which is usually defined as the maximum of the friction spike (*figure 1b*). Note that, at this point, the slider is already in motion and transiently reaches the loading velocity V , since (when inertia is negligible) $F(t) = K(Vt - x)$, where K is the stiffness of the loading spring.

Such studies, performed on a wide range of materials (paper, polymer glasses, elastomers), and focused on the fine variations of the friction coefficients, allow us to link macroscopic friction with the controlling physical mechanisms taking place on the micrometric scale of the real area of contact, and on the nanometric scale, within the adhesive contact layer.

2. The pinned interface

For low tangential loads ($F \ll F_s$), the shear displacement of the slider is fully reversible, hence elastic [4]. This regime corresponds to region (a) on *figure 2*, where the displacement x of the center of mass of the slider is plotted *versus* the tangential force.

The interfacial shear stiffness $\kappa = dF/dx$ measured in this linear regime is found to be proportional to the normal load and to obey an Amontons–Coulomb law:

$$\kappa = W/\lambda \quad (2)$$

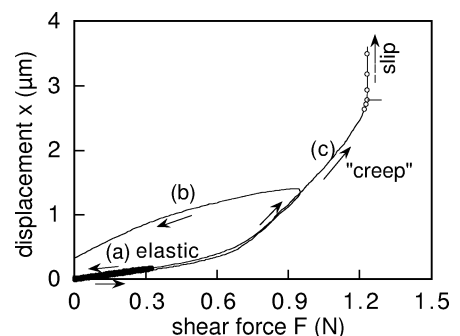
where λ is a length of micrometric order, thus giving an insight about the relevant scale for multicontact friction.

Since the order of magnitude of κ is much lower than the shear stiffness of the bulk of the slider and track, this elastic response must be attributed to the interfacial contact zone. Moreover, from experiments with various materials (paper, PMMA [poly(methyl methacrylate)], aluminium), λ is found to be weakly dependent on the elastic properties of the bulk.

This quite paradoxical feature can be qualitatively explained within the framework of Greenwood's model [2,4]. The shear stiffness of a single contact of size $\langle a \rangle$ is $\simeq G\langle a \rangle$ (with G the shear modulus). The interfacial stiffness $\kappa \simeq GN\langle a \rangle$, is thus proportional to the load W via the number of contacts. As a rule of thumb, the larger G , the larger the material hardness, and the smaller N . This is why, according to Greenwood, GN is quasi material independent, making λ a parameter of essentially topographic origin. For a roughness $\approx 1 \mu\text{m}$, one finds $\lambda \lesssim 1 \mu\text{m}$, to be compared with an average contact size $\langle a \rangle$ in the range 1–10 μm .

This elastic response in the pinned regime is also illustrated in *figure 3*. The frequency response of the slider to an oscillating shear force of small amplitude exhibits a well defined resonance [8], which is found, as expected, to occur at the circular frequency $2\pi f_0 = \sqrt{\kappa/M} = \sqrt{g/\lambda}$ (if the normal load is the weight of the slider $W = Mg$).

Figure 2. Loading–unloading characteristics of the slider–spring system for PMMA at 293 K. The spring of stiffness $K = 3 \cdot 10^4 \text{ N}\cdot\text{m}^{-1}$ is driven at $V = 10 \mu\text{m}\cdot\text{s}^{-1}$. (a) elastic response; (b) non-linear response with irreversible displacement; (c) full loading curve, from rest to slip, with transient creep motion.



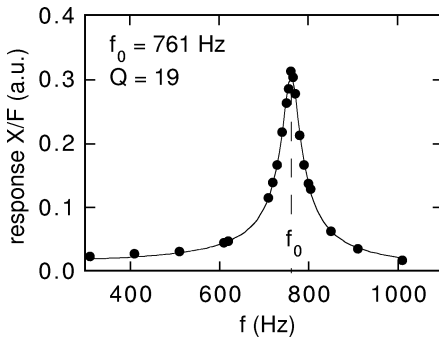


Figure 3. Frequency response to an oscillating shear force of a PMMA/PMMA interface at 293 K. x and F are the amplitude of displacement and shear force of the slider respectively. The full curve is fitted by the response of a single mass-spring-dashpot element of resonance frequency f_0 and quality factor Q .

In the example presented here, obtained with PMMA, the resonance frequency is $f_0 = 761$ Hz, which leads to a value of $\lambda = 0.4$ μm . Moreover, the quality factor of the resonance is $Q = 19$, in agreement with the viscoelastic loss angle of PMMA: $\tan \delta(f_0) \approx 1/Q$.

When the shear force is higher than, roughly, $0.5 F_s$, the response of the interface becomes non linear and a regime of creep motion is observed, resulting, as shown in *figure 2*, in an irreversible displacement when the force is decreased to zero. This creep regime, where frictional dissipation builds up, has been studied in detail via the response to an oscillating shear force of increasingly large amplitude [8].

3. Static threshold

Systematic experiments on various classes of materials show that μ_s exhibits a quasi logarithmic increase with the time of static contact τ prior to sliding (*figure 4*) [3,5,6,9]:

$$\mu_s(\tau) \approx \mu_s^0 + \beta_s \ln(\tau) \quad (3)$$

with $\beta_s \approx 10^{-2}$ at room temperature.

So, one must keep in mind that the static threshold is not an intrinsic property of a multicontact interface, but is protocol-dependent. When measuring it, one must specify τ and, also, the loading velocity: as already mentioned, μ_s is measured when the slider velocity reaches V .

The dependence of μ_s on the contact time can be quantitatively explained as resulting from the slow increase of the real area of contact through thermally activated creep of the load bearing asperities [5]. This accounts for most of the marked temperature dependence of the logarithmic slope β_s for PMMA/PMMA

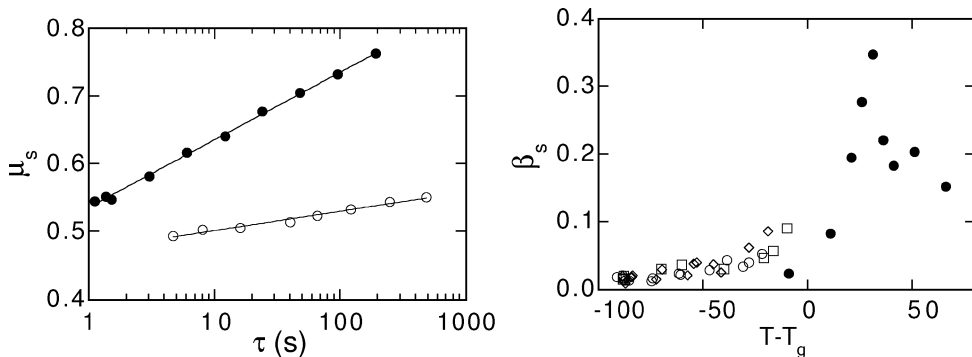


Figure 4. (a) Logarithmic increase of μ_s with the contact time τ , for PMMA at 293 K (\circ) and 345 K (\bullet). (b) Temperature dependence of the logarithmic slope β_s . Open symbols: PMMA glass; filled symbols: PI elastomer. Different symbols correspond to different samples. T_g is the glass transition temperature of each material.

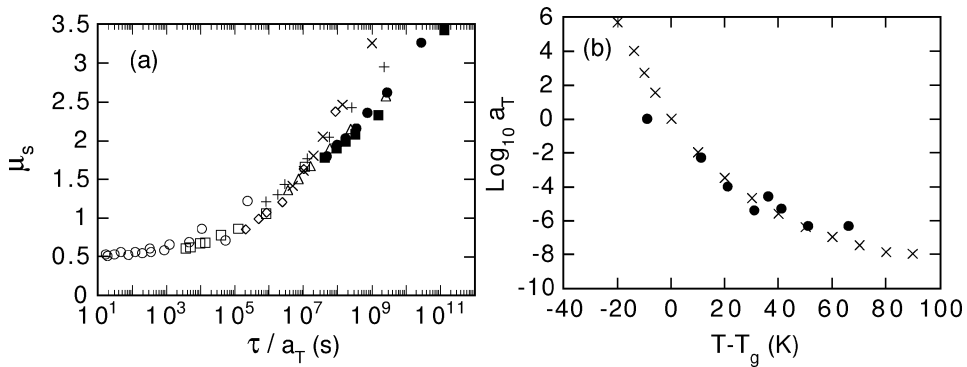


Figure 5. (a) Static friction coefficient μ_s versus reduced contact time τ/a_T (\circ 293 K; \square 313 K; \diamond 323 K; \times 333 K; $+$ 338 K; \triangle 343 K; \bullet 353 K; \blacksquare 368 K). (b) Shift factors derived from μ_s measurements (\bullet) compared with those from bulk measurements (\times).

interfaces (figure 4). However, note that for $T \sim T_g$, the characteristic shear strength σ_s itself might also become τ and T -dependent, due to polymer chain reptation at the polymer/polymer interface. A direct illustration of the creep growth of Σ_T has been provided by an in situ visualisation of the multicontact interface performed by Dieterich and Kilgore [10].

Above T_g , for a multicontact poly-isoprene (PI)/silica glass interface (where no reptation takes place) μ_s is found to obey a time-temperature equivalence of the WLF type (figure 5a) [6]:

$$\mu_s(\tau, T) = \mu_s(\tau/a_T) \quad (4)$$

The scaling factors a_T needed to obtain the μ_s master curve (figure 5b) agree with those derived from the WLF analysis of viscoelastic moduli of the bulk.

The logarithmic ageing of the static friction coefficient is thus the result of an increase of the real area of contact through either plastic or viscoelastic creep of the load bearing asperities.

4. The sliding interface

It is known from many studies that, in the low sliding velocity regime (typically $V < 100 \mu\text{s}^{-1}$), steady sliding of a multicontact interface is ‘velocity weakening’, i.e. $d\mu_d(V)/dV < 0$. For most materials which have been studied, one measures, to a good approximation:

$$\mu_d(V) \approx \mu_d^0 - \beta_d \ln(V) \quad (5)$$

with typically $\beta_d \approx 10^{-2}$.

Velocity-weakening friction is the source of the stick–slip instability: a fluctuation with, e.g., $\delta V > 0$ leads to a decrease of the friction force, hence to further acceleration.

4.1. Dynamical phase diagram

This argument might suggest that steady sliding is never stable. However, it is common knowledge that stick–slip does not occur when the pulling system is very stiff. This means that frictional dynamics is controlled, not only by the driving velocity V , but also by the stiffness K (figure 1), and, as we shall see, by the normal load W .

Using several contacting materials (paper, glassy PMMA and PS (polystyrene), rubber PI), we have shown [3,5] that the dynamical phase diagram (figure 6a) at low velocities ($V < 100 \mu\text{m}\cdot\text{s}^{-1}$) is generic.

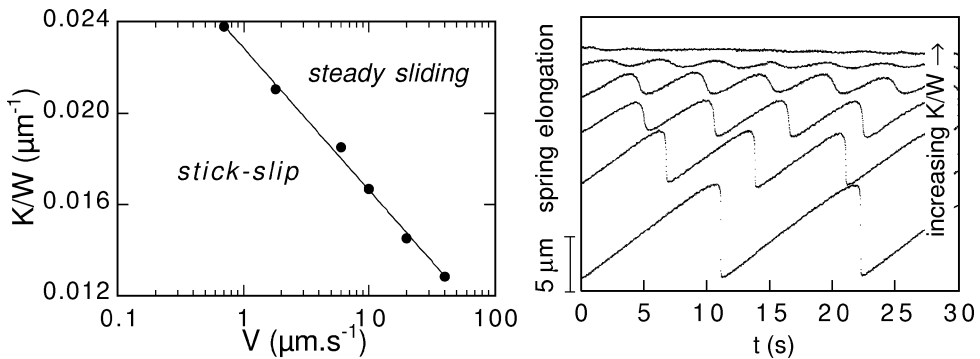


Figure 6. (a) Dynamical phase diagram for PMMA at 293 K. (b) Spring elongation versus time when K/W is increased at velocity $V = 1 \mu\text{m}\cdot\text{s}^{-1}$. An arbitrary vertical shift has been added to each trace for the sake of clarity.

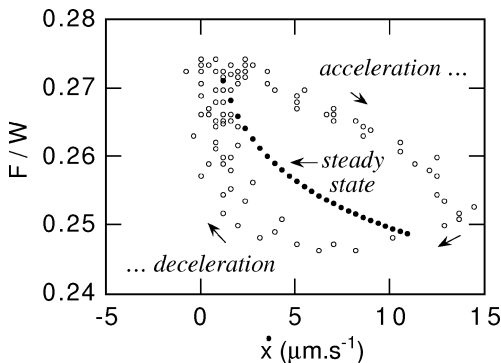


Figure 7. Hysteretic response to a slowly modulated driving velocity (\circ). The steady-state friction coefficient is shown in filled symbols.

Two regimes are found: for low V and low k (where $k = K/W$), periodic stick–slip is observed, whereas for high V and/or k , steady sliding occurs and a friction coefficient can be unambiguously defined. These two regions are separated by a bifurcation curve $k_c(V)$.

When the bifurcation curve is crossed, oscillatory motion appears: the amplitude of the oscillations increases continuously from zero at $k = k_c(V)$, while the harmonic content grows (*figure 6b*).

4.2. Transients in stable sliding

Within the stable sliding region of *figure 6*, the study of transient dynamics shows that, in non steady sliding, the friction coefficient is not simply a function of the instantaneous sliding velocity. Indeed, the response of the system to a slowly modulated driving velocity (acceleration and deceleration cycle) exhibits hysteresis (*figure 7*). This indicates that the instantaneous friction force depends on the dynamical history of the interface.

The study, by Dieterich, of the duration of the transient following a jump in driving velocity [9], has evidenced that this dynamical memory is interrupted after sliding a characteristic *length* D_0 , found again to be of micrometric order. All these results call for a model of non stationary friction.

4.3. State- and rate-dependent friction model

The results of the previous sections can be summed up as follows:

- The microcontacts undergo creep deformation under normal load, leading to logarithmic strengthening of the interface with its age Φ . By this we mean the average lifetime of a given set of microcontacts. In static experiments, Φ is the contact time τ .

- During sliding, the microcontacts population is refreshed after slipping, on average, the memory length D_0 . The interfacial ageing is thus interrupted by the sliding motion.
- So, in stationary sliding at velocity V , the average contact age reads $\Phi = D_0/V$, which decreases with increasing velocity and thus results in a velocity weakening contribution to μ_d .

In order to account phenomenologically for all these features, Rice and Ruina [11] proposed the following state- and rate-dependent friction model, in which the friction force reads:

$$F(\dot{x}, \Phi) = \mu_d W = W \left[\mu_0 + B \ln \left(\frac{\Phi}{\Phi_0} \right) + A \ln \left(\frac{\dot{x}}{V_0} \right) \right] \quad (6)$$

the evolution law of the state variable being:

$$\dot{\Phi} = 1 - \frac{\dot{x} \Phi}{D_0} \quad (7)$$

which interpolates between the static ($\Phi = t$) and the steady sliding ($\Phi = D_0/V$) cases.

The inertia-free equation of motion of the slider:

$$K(Vt - x) = \mu_d W \quad (8)$$

together with equations (6) and (7) provide a complete description of the non-linear friction dynamics.

We have used this model extensively [3,5] to analyse various types of dynamical transients, the dynamical phase diagram and the weakly nonlinear characteristics of stick–slip close to the bifurcation line. The overall agreement is excellent. Conversely, it is now possible to use systematically such an analysis of the dynamics to extract quantitatively the values of the various parameters of the model.

In particular, this method, applied to the temperature dependence of the frictional behaviour of PMMA/PMMA, has allowed us to propose an interpretation of the physical origin of the logarithmic velocity-strengthening contribution to μ_d (equation (6)) [5].

This results from the existence, within the nanometer-thick adhesive junction between contacting asperities, of bistable nanometric units which dissipate energy by suddenly flipping their configuration when a threshold stress is reached [12]. At finite temperature, flips occur before the spinodal limit of stability, due to thermal activation. This mechanism competes with the shear stress increase due to loading, thus resulting in the logarithmic junction rheology $A \ln(\dot{x})$ in equation (6). It is consistent with the temperature variation of the strengthening coefficient A .

5. Response to a normal load modulation: a mix of interface elasticity and rheology

In many situations of engineering or geophysical interest, frictional sliding occurs in the presence of a time-modulated normal load. We have studied the characteristics of the sliding motion with the following setup [7]: the slider is driven at constant V with $k > k_c(V)$, that is, in the absence of modulation, it would slide steadily; the normal load is modulated harmonically, $W = W_0(1 + \varepsilon \cos(2\pi ft))$, at $f = 120$ Hz and at amplitudes such that *no loss of contact occurs*.

Under such conditions, we measure a non harmonic oscillating shear force F that we characterize through its average value \overline{F} and its AC components at frequencies f and $2f$ (F_f and F_{2f} respectively).

The average friction coefficient $\overline{\mu}_d = \overline{F}/W_0$ is found to decrease substantially with increasing modulation amplitude, as shown in *figure 8*. Note that this nontrivial effect on the average shear force cannot be accounted for by an Amontons–Coulomb model ($F/W = Cst$), for which a harmonic modulation of W about W_0 results in a harmonic friction force of constant average value $\overline{F} = \mu_d W_0$. It thus reflects directly the dynamical variations of μ_d , as described by the state and rate model.

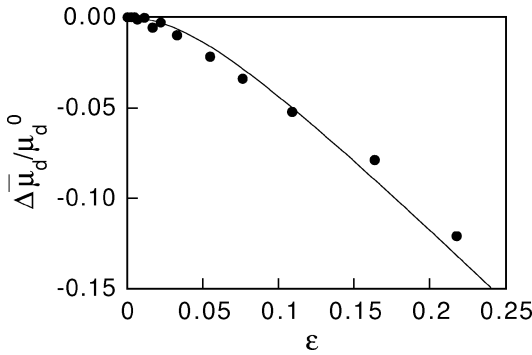


Figure 8. (●): relative variations of the average friction coefficient $\Delta\bar{\mu}/\mu_d^0 = (\bar{F}(\varepsilon) - F(0))/F(0)$ versus modulation amplitude, for PMMA at $f = 120$ Hz and 293 K. The solid line is the model prediction (see text).

However, the quantitative analysis of the ε -dependence of \bar{F} , F_f and F_{2f} shows that the state and rate equations (6)–(8), in which W becomes $W(t)$, must be extended as follows.

The rate variable that appears in the velocity-strengthening term must be understood as the rate of irreversible (plastic) deformation of the interfacial junction. As already mentioned in Section 2 the interface exhibits a tangential stiffness $\kappa = W/\lambda$, and can thus be pictured as an elastic element (the bodies of the asperities) in series with a sliding dissipative element (the nanometric junction). Therefore, the interfacial sliding speed is, strictly speaking:

$$\dot{x}_{\text{sliding}} = \frac{d}{dt} \left(x - \frac{F}{\kappa} \right) \quad (9)$$

where x is the position of the center of mass of the slider. In the presence of the load modulation, both F and κ are modulated, and the elastic deformation term in equation (9) becomes relevant.

This extended model yields an excellent overall agreement with the experimental data. For example, the theoretical curve in *figure 8* has been obtained without any parameter adjustment.

Moreover, we have studied extensively the effect of normal load modulation on the sliding stability, and found that load oscillations tend to stabilize sliding. That is, the bifurcation curve $k_c(V)$ (*figure 6a*) is shifted towards lower k , the shift increasing with the modulation amplitude. A description of this effect within the state and rate framework is now in progress [13].

It can easily be checked that the elastic correction (equation (9)), which of course does not contribute in stationary sliding, is negligible for weakly accelerated sliding motion, e.g. when analyzing the stick–slip bifurcation.

6. Conclusion

It is now clear that the dynamics of dry multicontact friction must be described by a friction coefficient depending not only on the instantaneous sliding velocity, but, also, on a dynamic state variable. This dependence on ‘state’ can be associated with the creep-growth of the real area of the micrometric contacts. The rate dependence of μ_d results from dissipation occurring on the nanometric scale within the interfacial adhesive junctions.

Let us insist that, in order to measure the state and rate parameters which govern the sliding dynamics, it is necessary to perform non-steady friction experiments. To this effect, quantitative analysis of the stick–slip instability, that requires non-standard tribometers with adjustable stiffness, has proved to be a powerful tool.

¹ Associé au Centre National de la Recherche Scientifique et aux universités Paris 6 et Paris 7.

References

- [1] Bowden F.P., Tabor D., *The Friction and Lubrication of Solids*, Clarendon, Oxford, 1950.
- [2] Greenwood J.A., Williamson J.B.P., Contact of nominally flat surfaces, *Proc. R. Soc. Lond. A* 295 (1966) 300.
- [3] Heslot F., Baumberger T., Perrin B., Caroli B., Caroli C., Creep, stick–slip, and dry friction dynamics: Experiments and a heuristic model, *Phys. Rev. E* 49 (1994) 4973.
- [4] Berthoud P., Baumberger T., Shear stiffness of a solid-solid multicontact interface, *Proc. R. Soc. Lond. A* 454 (1998) 1615.
- [5] Berthoud P., Baumberger T., G'Sell C., Hiver J.M., Physical analysis of the state- and rate-dependent friction law: Static friction, *Phys. Rev. B* 59 (1999) 14313;
Baumberger T., Berthoud P., Caroli C., Physical analysis of the state- and rate-dependent friction law. II. Dynamic friction, *Phys. Rev. B* 60 (1999) 3928.
- [6] Ronsin O., Labastie Coeyrehourcq K., State, rate and temperature-dependent sliding friction of elastomers, *Proc. R. Soc. London*, accepted.
- [7] Bureau L., Baumberger T., Caroli C., Shear response of a frictional interface to a normal load modulation, *Phys. Rev. E* 62 (2000) 6810.
- [8] Bureau L., Baumberger T., Caroli C., to be published.
- [9] Scholz C.H., *The Mechanics of Earthquakes and Faulting*, Cambridge University Press, Cambridge, England, 1990, Chapter 2.
- [10] Dieterich J., Kilgore B., Direct observation of frictional contacts: New insights for state-dependent properties, *Pure Appl. Geophys.* 143 (1994) 283.
- [11] Rice J.R., Ruina A.L., Stability of steady frictional slipping, *J. Appl. Mech.* 50 (1983) 343.
- [12] Persson B.N.J., *Sliding Friction: Physical Principles and Applications*, Nanosciences and Technology Ser., Springer Verlag, Berlin, 1998, Chapter 11.
- [13] Bureau L., Cochard A., unpublished.